NMR investigation of mechanically milled nanostructured GaF_3 powders

1999 J. Phys.: Condens. Matter 11 L423

(http://iopscience.iop.org/0953-8984/11/40/101)

J. Phys.: Condens. Matter **11** (1999) L423–L431. Printed in the UK PII: S0953-8984(99)06081-6

LETTER TO THE EDITOR

NMR investigation of mechanically milled nanostructured GaF_3 powders

B Bureau, H Guérault, G Silly, J Y Buzaré and J M Grenèche

Laboratoire de Physique de l'Etat Condensé, UPRES-A CNRS no 6087, Université du Maine, 72085 Le Mans Cedex 9, France

Received 15 July 1997

Abstract. High-energy ball milling is suitable for the preparation of nanostructured powders. First, high-resolution, solid-state nuclear magnetic resonance (NMR) investigations of ^{19}F, ^{69}Ga and ^{71}Ga in ball-milled ionic GaF_3 are presented. The quadrupolar parameter and the isotropic chemical shift distributions are determined for the three nuclei. The quadrupolar parameter distributions give clear evidence of two main structurally different phases in mechanically milled GaF_3. A discussion based upon molecular dynamics simulations allows us to distinguish these two phases according to the size of the distortion of the GaF_6 octahedral units: the lowest distortion is related to crystalline grains and the highest one to grain boundaries. It is thus concluded that NMR is a technique well adapted to the quantification and characterization of these two phases.

1. Introduction

Due to their potential applications in various areas (new alloys and ceramics, catalysts, high diffusivity materials, ...) there is a great interest in developing nanocrystalline materials [1–5]. These are polycrystalline powders with grain sizes of a few nanometres and a large interface fraction compared to that of the crystal. The grinding or ball-milling process is a well known method to reduce the size of the particles of various materials. Very often this technique is concerned with metallic materials. Generally, the structural and microstructural properties of the ball-milled powders are studied by x-ray diffraction (XRD) and transmission electron microscopy (TEM) [6]. These techniques characterize the grain size and its distribution. Since grinding of materials is a complex process depending on many factors, characterizations using all kinds of methods are needed for meaningful comparisons of experimental results. Local probe techniques can provide fruitful structural information because they are able to distinguish resonating species with different atomic environments. Over recent years, Mössbauer spectrometry [7–11] has shown its ability to estimate proportions of grains and grain boundaries in the case of nanocrystalline alloys containing appropriate probe nuclei.

The aim of this work is to demonstrate that solid-state nuclear magnetic resonance (NMR) is also well suited to the characterization of the ball-milled powders and to the study of the process of ball-milling. Because both crystalline and amorphous ionic fluoride phases behave as excellent model systems, we now concentrate our investigations on ball-milled ionic basic fluorides. Great attention has been focused on the compound GaF_3, because it contains three NMR active nuclei ^{19}F ($I = 1/2$) and $^{69,71}Ga$ ($I = 3/2$). In addition, the GaF_3 crystalline and amorphous related phases and PbF_2–ZnF_2–GaF_3 (PZG) glasses have

0953-8984/99/400423+09$30.00

been investigated recently by ^{19}F and $^{69,71}Ga$ solid-state NMR [12–15], which should allow informative comparisons. In particular, it has been shown that magic angle spinning (MAS) NMR of fluorine nuclei gives evidence for GaF_6 octahedra connectivity [12, 13] and NMR of quadrupolar Ga nuclei together with electric field gradient modelization are powerful tools to quantify the octahedron distortions [12, 14, 15]. Moreover, the NMR results on ball-milled GaF_3 have been compared to Mössbauer data obtained on the ball-milled ferric fluoride FeF_3 [16].

2. Experimental details

2.1. Materials

The mechanically milled GaF_3 phase was prepared from the rhombohedral crystalline phase of GaF_3 under an argon atmosphere in a commercial Fritsch Pulverisette 7 planetary ball-mill for 20 h at maximum power. Four zircon balls were used in each zircon vial with a powder-to-ball weight ratio of typically 1/30. The NMR rotors were filled in a controlled atmosphere to prevent the nanostructured powders from hydrolysis. An x-ray pattern was recorded to control the ball-milled GaF_3 structure. This enabled us to evidence the presence of crystalline grains, the sizes of which were estimated to be about 12–14 nm [16].

2.2. NMR measurements

The experiments were carried out at room temperature on a Bruker MSL 300 spectrometer (7.0 T). A commercial double bearing 4 mm MAS probe was used for static and MAS (15 kHz) spectra.

The unique ^{19}F isotope (abundance 100%) has a nuclear spin $I = 1/2$ and a good sensitivity (0.83). Its Larmor frequency is 282.282 MHz. The ^{19}F spectrum processing and acquisition parameters were identical to those used in the ^{19}F experiments in PZG glasses [13]: 15 kHz MAS, 7 μs single $\pi/2$ pulse duration for a uniform irradiation over a 100 kHz bandwidth, 1 s recycle time ($>5T_1$), spectral width 300 kHz, time domain 1024 points and 200 scans per spectrum. The measured isotropic chemical shift δ_{iso} is defined as $\delta_{ii} = \sigma_{ref} - \sigma_{ii}$, where σ_{ii} ($i = x, y, z$) are the principal components of the shielding tensor, σ_{ref} is the shielding tensor of the external reference C_6F_6 and $\delta_{iso} = \frac{1}{3}(\delta_{xx} + \delta_{yy} + \delta_{zz})$.

Both ^{69}Ga and ^{71}Ga isotopes have $I = 3/2$, their Larmor frequencies are 72.003 and 91.491 MHz and their quadrupole moments are $Q(^{69}Ga) = 0.17 \times 10^{-28}$ m^2 and $Q(^{71}Ga) = 0.11 \times 10^{-28}$ m^2, respectively. The definitions of the measured quadrupolar parameters are as follows. V_{XX}, V_{YY} and V_{ZZ} are the principal components of the electric field gradient tensor, with the condition $|V_{ZZ}| \geqslant |V_{YY}| \geqslant |V_{XX}|$ and $V_{ZZ} = eq$, the quadrupolar frequency is written as $\nu_Q = 3e^2qQ/2I(2I-1)h$ where Q is the quadrupolar moment and the asymmetry parameter is given by $\eta_Q = (V_{XX} - V_{YY})/V_{ZZ}$. The Ga isotropic chemical shift δ_{iso} is defined as above for ^{19}F. K_2NaGaF_6, in which the Ga atoms stand at the centre of regular octahedra [17], is used as an external reference. For six-fold coordinated Ga, it was previously shown that δ_{aniso} is negligible in comparison with ν_Q [18–20].

As in PZG glasses [14] and amorphous GaF_3 [15], the ^{69}Ga and ^{71}Ga static spectra in mechanically milled GaF_3 extend over more than 1 MHz due to the large quadrupolar interaction and it is thus impossible to irradiate uniformly the whole frequency range. The Ga spectra processing and acquisition parameters were similar to those used in previous experiments [14, 15]. Only the variable offset cumulative spectrum (VOCS [21]) technique together with full-echo acquisitions allowed us to acquire undistorted complete spectra. About

20 000 scans were necessary for each echo spectrum with a recycle delay of 250 ms. The radiofrequency field strength (100 kHz) was measured on a liquid containing Ga^{3+} ions (2.5 μs for $t_{\pi/2}$ liquid). The pulse length, t_{pulse}, was chosen to be much smaller than $t_{\pi/2}$ ($t_{\pi/2} \approx 3.5\, t_{pulse}$) to ensure a linear irradiation regime in order to avoid the distortion of the central transition [22, 23].

3. Results

3.1. ^{19}F MAS NMR

The ball-milled GaF_3 ^{19}F spectrum is compared in figure 1 with those obtained in crystalline and amorphous GaF_3 [12, 13]. The ^{19}F MAS NMR spectra were recorded at 15 kHz spinning speed; then the chemical shift was averaged and the strong dipolar interaction between ^{19}F nuclei was reduced. Due to the MAS rotation, some spinning side bands appear (labelled * in figure 1) at 15 kHz around the actual central fluorine line. The ^{19}F isotropic chemical shift in the two disordered GaF_3 phases is equal to the value measured in the crystalline GaF_3: $\delta_{iso} = -3$ ppm [12, 13]. The structural disorder affects only the linewidths: the isotropic line is larger in the ball-milled GaF_3 (4.8 kHz) than in the crystalline phase (3.3 kHz), but thinner than in the amorphous one (8.6 kHz).

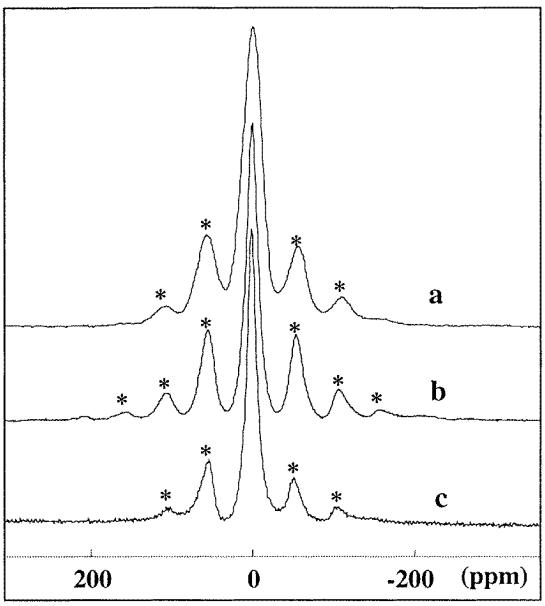

Figure 1. ^{19}F MAS NMR spectra of amorphous (a), ball-milled (b) and crystalline (c) GaF_3 recorded at 15 kHz. The lines labelled * are spinning side bands.

3.2. $^{69,71}Ga$ static NMR

As previously observed in amorphous GaF_3 and PZG glasses [12, 14, 15], the ^{69}Ga spectra are simply deduced from the ^{71}Ga corresponding ones by a multiplication of the frequency scale by a factor 3.2. Therefore, in the following, only ^{71}Ga spectra will be shown and discussed. In figure 2, the ball-milled ^{71}Ga static NMR spectrum is compared with those obtained in

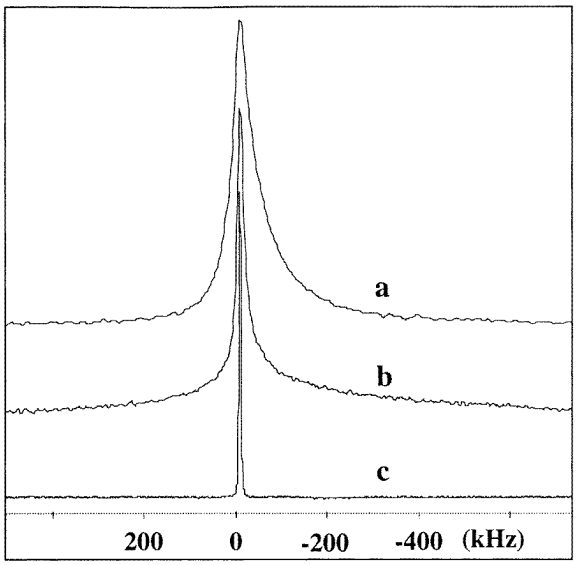

Figure 2. ^{71}Ga NMR spectra of amorphous (a), ball-milled (b) and crystalline (c) GaF_3.

crystalline and amorphous GaF_3. As for ^{19}F, at first sight, the structural disorder induced by the ball-milling process only affects the linewidth and its value is intermediate between those observed in crystalline and amorphous GaF_3, respectively.

In PZG glasses [14], as in amorphous GaF_3 [15], the strongly asymmetric broad line without any resolved structure was simulated using a unique quadrupolar parameter distribution $P(\nu_Q, \eta_Q)$ established by Czjzek *et al* in the case of a dense random packing of hard spheres [24, 25]. The $P(\nu_Q, \eta_Q)$ expression may be written as

$$P(\eta_Q, \eta_Q) = \frac{1}{\sqrt{2\pi}\sigma^d}\nu_Q^{d-1}\eta(1-\eta_Q^2/9)\exp\left\{-\frac{\nu_Q^2(1+\eta_Q^2/3)}{2\sigma^2}\right\}$$

where σ and d are two adjustable parameters.

Simulations of both ^{69}Ga and ^{71}Ga NMR spectra were performed using a modified version of the WINFIT Bruker software package developed by Massiot *et al* [26] who introduced Czjzek's distribution in the program: details about simulations applied to disordered fluorides using the $P(\nu_Q, \eta_Q)$ distribution can be found in [14].

In contrast to amorphous GaF_3 or PZG glass, an unique Czjzek's distribution did not allow us to reconstruct the ^{69}Ga and ^{71}Ga static spectra of ball-milled GaF_3. It was necessary to introduce a second distribution. The best fit obtained by using two distributions with 400 pairs of quadrupolar parameters (ν_Q, η_Q) is presented in figure 3. The corresponding ^{71}Ga parameters are as follows: for the broad contribution, the relative intensity is 0.7, $d = 3$, $\sigma = 4900 \pm 100$ kHz; for the sharp one the relative intensity is 0.3, $d = 3, \sigma = 1100 \pm 100$ kHz; the isotropic chemical shift is $\delta_{iso} = -60 \pm 10$ ppm for both contributions. For ^{69}Ga, the chemical shifts are identical and the σ values have to be multiplied by 1.55 (the ratio of the quadrupole moments).

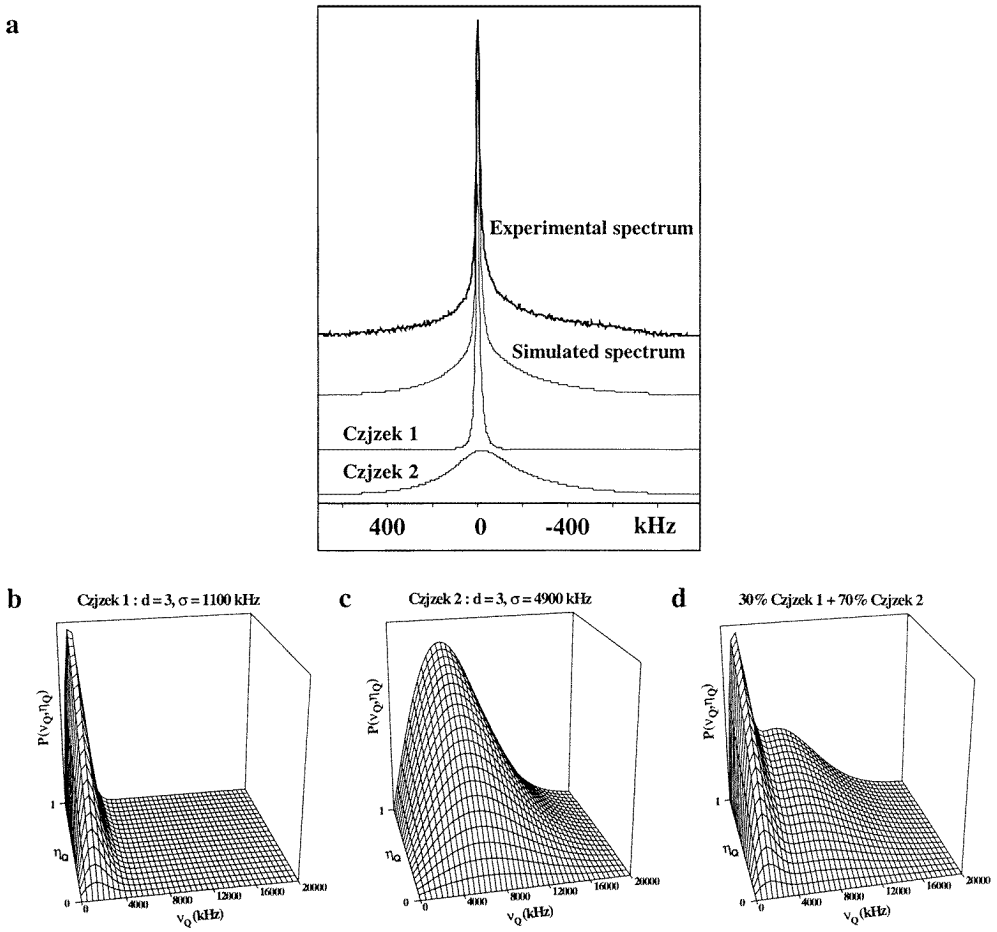

Figure 3. Experimental and simulated ^{71}Ga NMR spectra (a), the calculated spectra is the weighted sum of the two spectra obtained from Czjzek's distributions. Czjzek's distributions used to calculate the simulated spectra: (b) $d = 3$, $\sigma = 1100$ kHz; (c) $d = 3$, $\sigma = 4900$ kHz. (d) Total quadrupolar parameter distributions with 30% of the thin Czjzek's distribution plus 70% of the broader one.

4. Discussion

In such mechanically milled powders, two contributions called grains and grain boundaries are generally expected [27]: the grain structure is not far from the structure of the starting material (crystalline GaF_3), whereas the grain boundary is much more affected by the ball-milling and its structure should be close that of amorphous GaF_3. The Ga NMR spectra are in agreement with this model. The σ parameter of the broad Czjzek's distribution (4900 kHz) is larger than the one found for the amorphous GaF_3 (3500 kHz [12, 15]). So, on average, the related fluorine octahedra are somewhat more strongly distorted than in the amorphous phase and so are attributed to the grain boundaries. On the other hand, the small σ parameter of the sharp Czjzek's distribution (1100 kHz) is related to octahedra which are somewhat slightly more distorted than that obtained in crystalline GaF_3 ($\nu_Q = 500$ kHz [12, 15]): these octahedra are expected to belong to the crystalline grains.

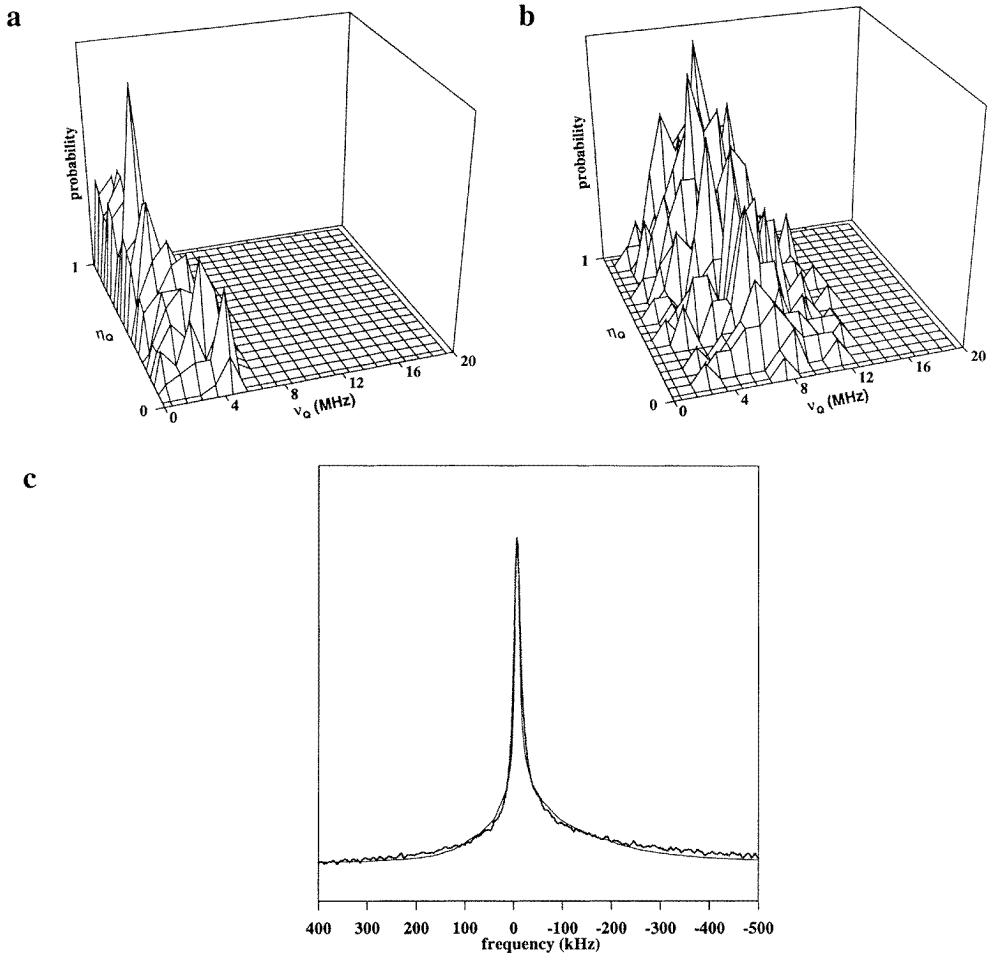

Figure 4. Quadrupolar parameter distributions and related simulated NMR spectra calculated from molecular dynamics data at (a) '10 K' and (b) '300 K' with $\alpha_e(F^-) = 1.75$ Å^3. (c) The experimental spectrum (thick full curve) is compared to the calculated one (thin full curve).

The chemical shift value of both contributions ($\delta_{iso} = -60 \pm 10$ ppm) is typical of a six-fold fluorine coordinated gallium [14, 15]. This result proves that the ball-milling process does not break the octahedral entities. Furthermore, the crystalline rhombohedral and amorphous GaF_3 networks are built up from corner-sharing $(GaF_6)^{3-}$ octahedra [15, 27]. The ^{19}F isotropic chemical shift (-3 ppm) measured in these compounds is typical of F^- ions shared between two fluorine octahedra centred on Ga^{3+} ions [13]. In contrast to PZG glasses, neither unshared nor free fluorines whose chemical shifts would be about 70 ppm and 150 ppm, respectively, in such fluorine compounds [13] are observed. Finally, we may infer that the ball-milled GaF_3 network is built up from corner-sharing $(GaF_6)^{3-}$ octahedra.

In a previous work [12, 15], we have shown that it is possible to quantify the radial and angular octahedron distortions in amorphous GaF_3 by performing electric field gradient (EFG) calculations. The results were found to be strongly dependent on the F^- ion polarizability denoted as $\alpha_e(F^-)$: the larger α_e (F^-) is, the higher the calculated quadrupolar frequencies and the broader the related calculated NMR spectra.

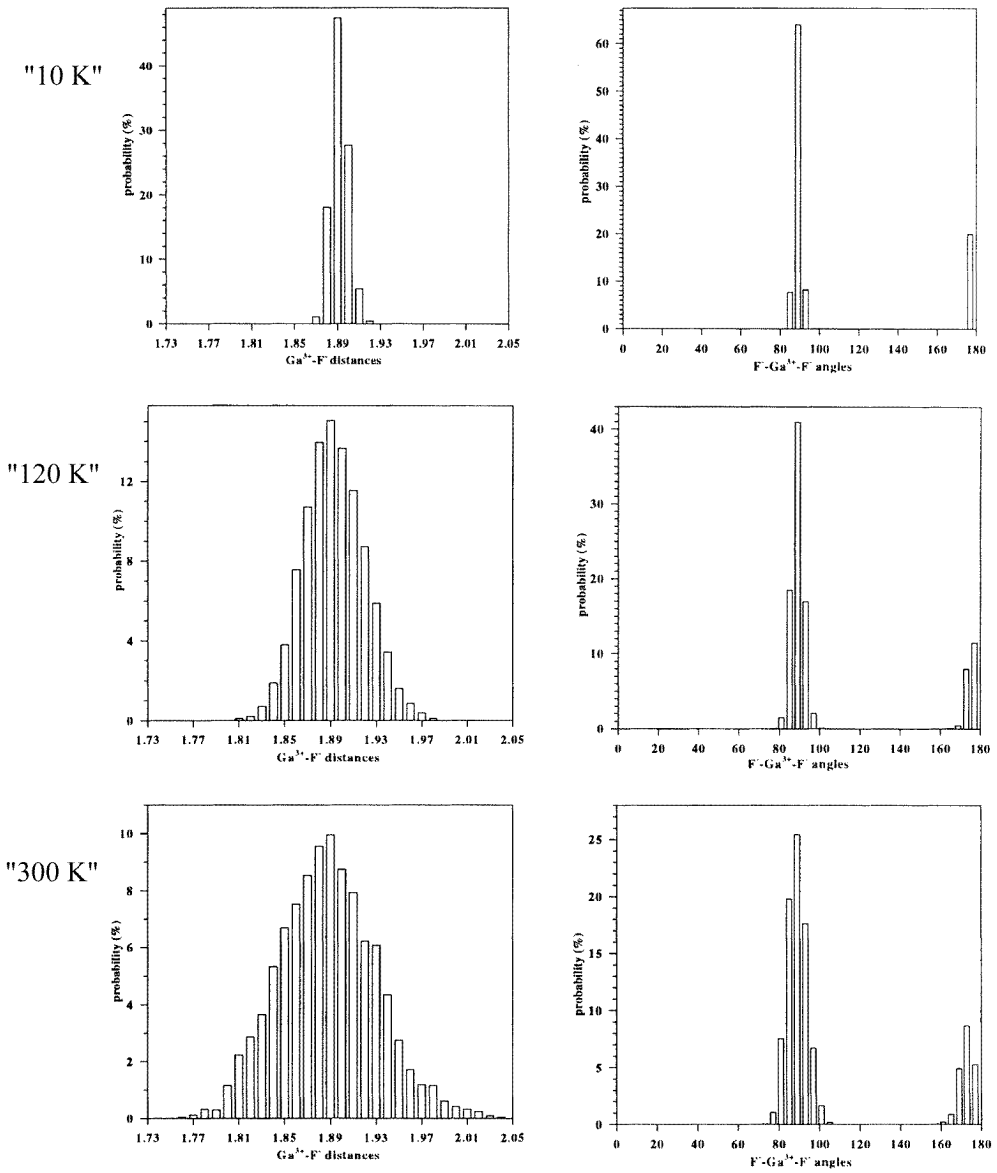

Figure 5. Ga–F distance and F–Ga–F angle distributions in $(GaF_6)^{3-}$ octahedra obtained by molecular dynamics calculations at '10 K', '120 K' and '300 K' starting from the rhombohedral GaF_3 phase.

The amorphous GaF_3 octahedron distortions were simulated by using molecular dynamics calculations starting from the crystalline rhombohedral GaF_3 [12, 15]. The 'temperature *T*' is the relevant parameter of the calculation. It fixes the total energy of the system. The higher it is, the faster the ions move and the larger the generated octahedron distortions [29]. A previous EPR study has shown that the amorphous GaF_3 octahedra were slightly distorted and that the atomic position data files obtained at '120 K' gives a good account for the EPR spectra [29]. The same conclusion was obtained in NMR using 1.75 $Å^3$ for the F^- ion polarizability [12, 15]. This value is not far from 1.62 $Å^3$ recently calculated by Shannon [30]. So, in order to simulate

Table 1. Mean values and standard deviations (st. dev.) of the radial and angular distributions obtained by molecular dynamics simulations: '10 K' corresponds to the grain, '120 K' to the amorphous GaF_3 and '300 K' to the grain boundaries. $\langle\alpha\rangle$ and $\langle\beta\rangle$ stand for mean values of the two kinds of F–Ga–F angles in GaF_6 octahedra.

	$\langle d_{Ga-F}\rangle$ (Å)	Radial st. dev. (Å)	$\langle\alpha\rangle$ (°)	st. dev. from 90° (°)	$\langle\beta\rangle$ (°)	st. dev. from 180° (°)
'10 K'	1.887	0.008	90.00	1.51	178.1	2.27
'120 K'	1.888	0.026	89.99	3.00	175.7	4.84
'300 K'	1.893	0.042	89.98	4.83	173.0	7.89

the structure of the two ball-milled GaF_3 phases, we also use this polarizability value. The atomic position data files obtained at '10 K' and '300 K' enable us to reach a good agreement with the thin and large contributions of the experimental spectrum, respectively. The calculated quadrupolar parameter distributions are illustrated in figures 4(a) and 4(b) and the total simulated spectrum is compared with the experimental one on figure 4(c). Figure 5 displays the octahedron distortion distributions at '10 K' (grain), '120 K' (amorphous phase) and '300 K' (grain boundary): 80% of the angles F–Ga–F (labelled α in table 1) are distributed around 90° and 20% of the angles F–Ga–F (labelled β in table 1) near 180°. Table 1 compares the mean values and the standard deviations of the radial and angular distributions obtained for amorphous GaF_3, the grains and the grain boundaries of ball-milled GaF_3: the octahedra of the grains are only slightly distorted whereas those of the grain boundaries are more distorted than in amorphous GaF_3.

It is important to emphasize the high sensibility of NMR in studying quadrupolar nanostructured systems, through short-range quadrupolar interaction (first neighbours). In addition to an estimate of the crystalline fraction in these nanostructured fluorides, NMR reveals the presence of slightly distorted $(GaF_6)^{3-}$ octahedra within crystalline grains. This weak local disorder probably originates from the presence of microstresses mechanically introduced during the ball-milling process, which is also pointed out by x-ray pattern analysis [16]. Such small effects might be evidenced by Mössbauer spectrometry on quadrupolar systems. Nevertheless, this technique is widely applied to iron-based magnetic systems, which prevents the detection of local distortions because the magnetic interactions completely dominate the quadrupolar effects in ferric or metallic systems. In other respects, diffraction techniques average structural data over the coherent diffraction volume.

5. Conclusion

Using different acquisition techniques, ^{19}F, ^{69}Ga and ^{71}Ga NMR spectra were recorded in ball-milled GaF_3. From the relevant chemical shift values, it appears that the ball-milled GaF_3 network is built up from corner-sharing $(GaF_6)^{3-}$ octahedra. To account for the ^{69}Ga and ^{71}Ga NMR spectra in ball-milled GaF_3, two Czjzek's distributions were necessary, which indicates the existence of two phases: the narrow distribution was attributed to the grains whose structure is not far from that of the starting crystalline GaF_3, and the larger one was associated with the grain boundaries which are more affected by the ball-milling. The relative intensities of these two contributions allowed us to estimate the proportions of both the grains (30%) and grain boundaries (70%). Finally, it was possible to quantify the octahedron distortions as previously done in amorphous GaF_3. In the grain the $(GaF_6)^{3-}$ octahedra are very slightly distorted, whereas in the grain boundaries the $(GaF_6)^{3-}$ octahedron distortions are larger than those observed in amorphous GaF_3.

References

[1] Gleiter H and Marquardt P 1984 *Z. Metall.* **75** 263
[2] Birringer R, Herr U and Gleiter H 1986 *Trans. Japan Inst. Metals Suppl.* **27** 43
[3] Fecht H J, Hellstern E, Fu Z and Johnson W L 1990 *Metall. Trans.* A **21** 2333
[4] Eckert J, Holzer J C, Krill C E III and Johnson W L 1992 *J. Mater. Res.* **7** 1751
[5] Morris M A and Morris D G 1991 *J. Mater. Sci.* **26** 4687
[6] Du Y J, Guo F Q and Lu K 1996 *Nanostruc. Mater.* **7** 579
[7] Le Caer G, Delcroix P, Shen T D and Malaman B 1996 *Phys. Rev.* B **54** 12 775
[8] Le Caer G and Delcroix P 1997 *Czech. J. Phys.* **47** 489
[9] Miglierini M and Greneche J M 1997 *J. Phys.: Condens. Matter* **9** 2303
[10] Slawska-Waniewska A and Greneche J 1997 *Phys. Rev.* B **56** 8491
[11] Greneche J M 1999 *Mater. Sci. Forum* **307** 159
[12] Bureau B 1998 *Thesis* Université du Maine, Le Mans, France
[13] Bureau B, Silly G, Buzaré J Y, Emery J, Legein C and Jacoboni C 1997 *J. Phys.: Condens. Matter* **9** 6719
[14] Bureau B, Silly G, Buzaré J Y, Legein C and Massiot D *Solid State NMR* at press
[15] Bureau B, Silly G, Buzaré J Y, Boulard B and Legein C *Phys. Rev.* B, submitted
[16] Guérault H and Greneche J M, to be published
[17] Haegele R, Verscharen W and Babel D 1977 *Z. Anorg. Allg. Chem.* **2** 1947
[18] Massiot D, Farnan I, Gautier N, Trumeau D, Trokiner A and Coutures J P 1995 *Solid State NMR* **4** 241
[19] Vosegaard T, Massiot D, Gautier N and Jakobsen H 1997 *Inorg. Chem.* **36** 2446
[20] Vosegaard T, Byriel I P, Binet L, Massiot D and Jakobsen H 1998 *J. Am. Chem. Soc.* **120** 8184
[21] Massiot D, Farnan I, Gautier N, Trumeau D, Florian P and Grandinetti P J 1995 *J. Chem. Phys.* **92** 1847
[22] Man P P 1986 *J. Magn. Reson.* **67** 78
[23] Man P P 1993 *Appl. Magn. Reson.* **4** 65
[24] Czjzek G, Fink J, Gotz F, Schmidt H, Coey J M D, Rebouillat J P and Liénard A 1981 *Phys. Rev.* B **23** 2513
[25] Czjzek G 1982 *Phys. Rev.* B **25** 4908
[26] Massiot D, Thiele H and Germanus A 1994 *Bruker Rep.* **140** 43
[27] Gleiter H 1989 *Prog. Mater. Sci.* **33** 223
[28] Brewer F M, Garton G and Goodgame D M L 1959 *J. Inorg. Nucl. Chem.* **9** 56
[29] Legein C, Buzaré J Y, Boulard B and Jacoboni C 1995 *J. Phys.: Condens. Matter* **7** 4829
[30] Shannon R D 1993 *J. Appl. Phys.* **73** 348